Journal of Sound and Vibration (1994) **169**(1), 19–28

A CLOSED FORM SOLUTION OF A LONGITUDINAL BAR WITH A VISCOUS BOUNDARY CONDITION

A. J. HULL

Submarine Sonar Department, Naval Undersea Warfare Center, New London, Connecticut 06320, *U.S.A.*

(*Received* 13 *April* 1992, *and in final form* 7 *July* 1992)

A closed form solution of a longitudinal bar with a viscous boundary condition subjected to point loading is developed in this paper. A new series solution is formulated that allows the time and space modes of the beam to decouple. This expansion yields explicit eigenvalues and eigenvectors. A frequency domain example is presented, and the results are compared with finite element solutions of the same problem. It is shown that the closed form solution is computationally more efficient than a finite element solution. Additionally, the truncation error at lower frequencies is shown to be extremely small. The method is easily implemented, and can provide time and frequency domain solutions to this class of problems.

1. INTRODUCTION

The dynamic response of a bar with a viscous boundary condition is important because the designers of various structures often use viscous dampers to reduce force transmissibility and decrease displacement. The need for reduced force transmissibility is evident since lower force levels permit simpler and lighter structural designs. For this reason, viscous (shock) absorbers are currently critical to many systems, such as buildings, cars and airplanes.

The closed form response of structures with fixed and free boundary conditions has been previously analyzed [1–3]. These analyses form the basis for many classical beam problems. Their self-adjoint operators are discretized using mutually orthogonal modes to produce models of structural dynamic response. However, these models admit only standing waves into the response and do not consider viscous damping at the boundary. Recently, a number of papers have appeared that model different effects in beams, such as compressive axial loads [4, 5], elastic foundations [6], and the coupling between flexural and torsional modes to axial loads [7]. In these papers, which use a variety of analytical techniques to solve for the structural response of a beam, viscous dissipation at the boundary is not considered.

Although the structural response of a bar with a viscous damper can be determined using a finite element analysis [8, 9], this method does have a number of drawbacks. It is computationally intensive, does not provide explicit eigenvalues and eigenvectors, and does not yield a closed form solution. Finite element discretizations are often too large when real time computations are required, as in the case of active control systems. Additionally, the effects of changing model parameters is not always as apparent in a finite element model as it is in a closed form algebraic solution.

0022-460X/94/010019 + 10 $08.00/0

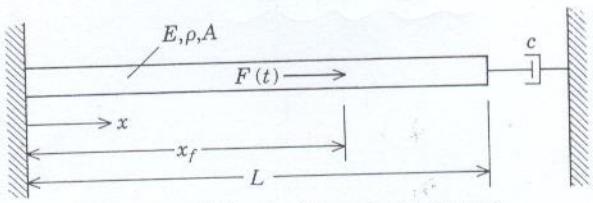

Figure 1. The beam with a viscous damper.

In this paper, a closed form series solution is developed for the axial wave equation with a fixed boundary condition at one end and a viscously damped boundary condition at the other. The addition of a damper to the boundary allows propagating and standing waves to exist in the structure simultaneously. The system model produces a differential operator that is non-self-adjoint and corresponding eigenfunctions that are not mutually orthogonal (with a weight function of unity or on the original problem definition interval). By redefinition of the problem on another interval, the space and time modes will decouple and a closed form series solution can be found.

2. SYSTEM MODEL

The system model represents an axial bar fixed at $x = 0$ and a viscous damper at $x = L$ (Figure 1). A force is applied to the bar at location $x = x_f$. The addition of the damper to the bar will admit standing and propagating wave energy simultaneously. The linear second order wave equation modelling particle displacement in the bar is

$$\frac{\partial^2 u(x,t)}{\partial t^2} - \frac{E}{\rho}\frac{\partial^2 u(x,t)}{\partial x^2} = \frac{\delta(x - x_f)F(t)}{\rho A}, \tag{1}$$

where $u(x, t)$ is the displacement (m), E is the modulus of elasticity (N/m^2), ρ is the density of the bar (kg/m^3), x is the spatial location (m), t is time (s), A is the area of the bar (m^2), F is the applied force (N), and δ is the Dirac delta function (1/m). The wave equation assumes uniform area and negligible internal loss in the bar.

The boundary at $x = 0$ is fixed and can be expressed as

$$u(0, t) = 0. \tag{2}$$

The boundary condition $x = L$ is obtained by matching the force at the end of the bar to the viscous dissipative force of the damper. This can be expressed as

$$AE\frac{\partial u}{\partial x}(L, t) = -c\frac{\partial u}{\partial t}(L, t), \tag{3}$$

where c is the viscous damping coefficient (Ns/m). When c is equal to zero (or infinity), the boundary at $x = L$ reflects all the wave energy, and the system response is composed only of standing waves. When c is equal to $A\sqrt{\rho E}$, the boundary at $x = L$ absorbs all the wave energy, and the system response is composed only of propagating waves. All other values of c exhibit some combination of standing and propagating wave energy in their response.

3. SEPARATION OF VARIABLES

A decoupled series of ordinary differential equations that represents the system is now developed from equations (1)–(3) and the initial conditions of the bar. The first step

in deriving decoupled differential equations involves finding the eigenvalues and eigenfunctions of the model. This is accomplished by application of separation of variables to the homogenous version of the wave equation (equation (1)) and the corresponding boundary conditions (equations (2) and (3)). Separation of variables assumes that the independent variable can be written as a product of two functions—one in the time domain and one in the spatial domain. This form is

$$u(x, t) = T(t)X(x). \tag{4}$$

Equation (4) is now substituted into the homogeneous version of equation (1), which produces the ordinary differential equations

$$\frac{\mathrm{d}^2T(t)}{\mathrm{d}t^2} - \lambda^2 \frac{E}{\rho} T(t) = 0 \tag{5}$$

and

$$\frac{\mathrm{d}^2X(x)}{\mathrm{d}x^2} - \lambda^2 X(x) = 0, \tag{6}$$

where λ is the complex-valued separation constant.

The general solution to equation (5) is

$$T(t) = G\,\mathrm{e}^{\lambda\sqrt{E/\rho}t} + H\,\mathrm{e}^{-\lambda\sqrt{E/\rho}t}. \tag{7}$$

The fixed boundary condition (equation (2)), is now applied to the spatial ordinary differential (equation (6)) which gives

$$X(x) = \mathrm{e}^{\lambda x} - \mathrm{e}^{-\lambda x}. \tag{8}$$

Applying the viscous boundary condition (equation (3)) to equations (7) and (8) yields $H = 0$ and the n-mode-indexed separation constant

$$\lambda_n = \frac{1}{2L} \log_{\mathrm{e}}\left[\frac{AE - c\sqrt{E/\rho}}{AE + c\sqrt{E/\rho}}\right] + \frac{(2n+1)\pi}{2L}\mathrm{i}, \qquad n = 0, \pm 1, \pm 2, \ldots, \tag{9}$$

where $\mathrm{i} = \sqrt{-1}$. The real part of the separation constant is associated with the propagating wave energy, and the imaginary part of the separation constant is associated with the standing wave energy. The eigenvalues of the system are the separation constants multiplied by the wave speed,

$$\Lambda_n = \sqrt{E/\rho}\,\lambda_n, \tag{10}$$

where Λ_n has units of rad/s. A plot of the eigenvalue location in the complex plane is shown in Figure 2. The eigenvalues are equally spaced and parallel to the imaginary axis. Once the indexed separation constant is determined, the spatial eigenfunctions can be defined by inserting equation (9) into equation (8), which gives

$$\varphi_n(x) = \mathrm{e}^{\lambda_n x} - \mathrm{e}^{-\lambda_n x}. \tag{11}$$

A typical eigenfunction ($n = 2$) is shown in Figure 3 for $c = (0{\cdot}5)A\sqrt{\rho E}$. The eigenfunctions are not mutually orthogonal on $[0, L]$; therefore their integral with respect to one another on $[0, L]$ is not zero, and traditional boundary value techniques will not decouple the time and space modes. A method is developed below that redefines the problem interval over $[-L, L]$ and decouples the time and space modes of the system. Once the modes have

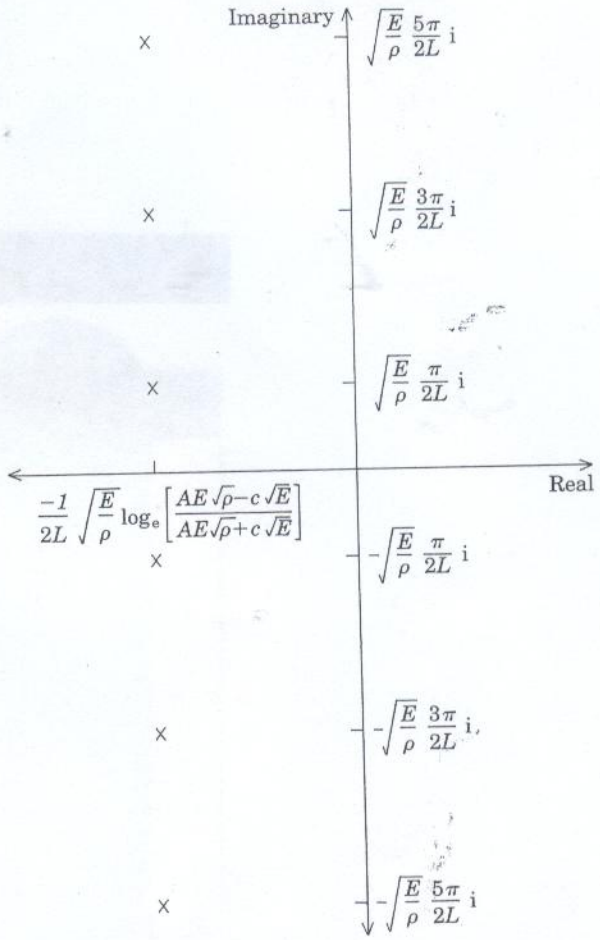

Figure 2. The eigenvalue location in the complex plane.

been decoupled, the problem solution can be transformed back to the original interval of $[0, L]$.

4. SERIES SOLUTION

The displacement (or solution) to the forced wave equation, written as a series solution, is

$$u(x, t) = \sum_{n=-\infty}^{\infty} b_n(t)\varphi_n(x), \tag{12}$$

where the $b_n(t)$'s are the generalized co-ordinates and the $\varphi_n(x)$'s are the spatial eigenfunctions. Derivation of a solution that decouples the time and space modes requires the time derivative (velocity) of the particle displacement to be written in two different forms. The first form is the derivative of equation (12) and yields

$$\frac{\partial u}{\partial t}(x, t) = \sum_{n=-\infty}^{\infty} \dot{b}_n(t)\varphi_n(x), \tag{13}$$

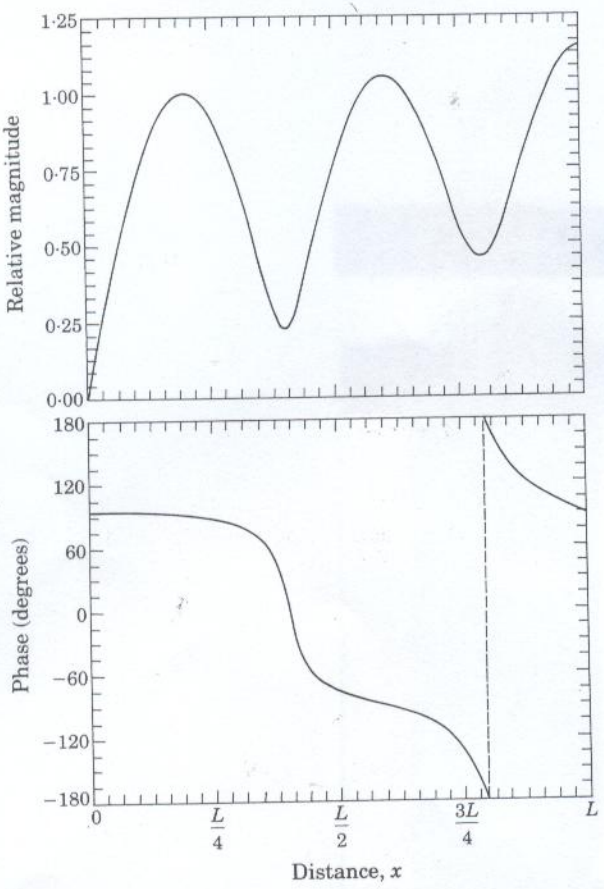

Figure 3. The $n = 2$ eigenfunction with $c = (0{\cdot}5)A\sqrt{\rho E}$: (a) relative magnitude; (b) phase.

where the dot over b denotes the time derivative of the function. The second, developed by using equations (7) and (4), is written as

$$\frac{\partial u}{\partial t}(x, t) = \sum_{n=-\infty}^{\infty} \Lambda_n b_n(t)\varphi_n(x). \tag{14}$$

Equating equations (13) and (14) produces

$$\sum_{n=-\infty}^{\infty} [\dot{b}_n(t) - \Lambda_n b_n(t)]\varphi_n(x) = 0. \tag{15}$$

The assumption is now made that differentiation will distribute over the summation. Decoupled space and time modes will validate this assumption. The forced wave equation (1) is rewritten with the above equations. The second partial time derivative is found from the time derivative of equation (14), and the second partial spatial derivative is found from the second spatial derivative of equation (13). Inserting these derivatives into equation (1) yields

$$\sum_{n=-\infty}^{\infty} [\dot{b}_n(t) - \Lambda_n b_n(t)]\Lambda_n \varphi_n(x) = \delta(x - x_f)F(t)/(\rho A). \tag{16}$$

Equation (15) is now differentiated with respect to x and multiplied by the wave speed $\sqrt{E/\rho}$. The result is then added to equation (16) to form

$$\sum_{n=-\infty}^{\infty} [\dot{b}_n(t) - \Lambda_n b_n(t)] 2\Lambda_n \, e^{i\lambda_n x} = \delta(x - x_f)F(t)/(\rho A), \qquad x \in [0, L], \tag{17}$$

and is subtracted from equation (16) to give

$$\sum_{n=-\infty}^{\infty} [\dot{b}_n(t) - \Lambda_n b_n(t)] 2\Lambda_n \, e^{-i\lambda_n x} = -\delta(x - x_f)F(t)/(\rho A), \qquad x \in [0, L]. \tag{18}$$

The interval of equation (18), now changed from $[0, L]$ to $[-L, 0]$ by substitution of $-x$ for x, yields

$$\sum_{n=-\infty}^{\infty} [\dot{b}_n(t) - \Lambda_n b_n(t)] 2\Lambda_n \, e^{i\lambda_n x} = -\delta(-x - x_f)F(t)/(\rho A), \qquad x \in [-L, 0]. \tag{19}$$

Combining equations (17) and (19) into a single equation and breaking the exponential into terms that contain the index n and terms that do not contain the index n results in

$$\sum_{n=-\infty}^{\infty} [\dot{b}_n(t) - \Lambda_n b_n(t)] 2\Lambda_n \, e^{(2n+1)\pi x i/(2L)}$$

$$= \begin{cases} \exp\left\{\dfrac{-1}{2L} \log_e \left[\dfrac{AE\sqrt{\rho} - c\sqrt{E}}{AE\sqrt{\rho} + c\sqrt{E}}\right] x\right\} \left[\dfrac{-\delta(-x - x_f)F(t)}{\rho A}\right], & x \in [-L, 0], \\ \exp\left\{\dfrac{-1}{2L} \log_e \left[\dfrac{AE\sqrt{\rho} - c\sqrt{E}}{AE\sqrt{\rho} + c\sqrt{E}}\right] x\right\} \left[\dfrac{\delta(x - x_f)F(t)}{\rho A}\right], & x \in [0, L]. \end{cases} \tag{20}$$

The exponential $e^{-(2m+1)\pi x i/(2L)}$ (where m is an integer) is now multiplied on both sides of equation (20), and the resulting equation is integrated from $-L$ to L. The left side of the equation can be expressed as

$$\int_{-L}^{L} [\dot{b}_n(t) - \Lambda_n b_n(t)] 2\Lambda_n \, e^{(2n+1)\pi x i/(2L)} e^{-(2m+1)\pi x i/(2L)} \, dx$$

$$= \begin{cases} [\dot{b}_n(t) - \Lambda_n b_n(t)] 4L\Lambda_n, & n = m, \\ 0, & n \neq m. \end{cases} \tag{21}$$

Use of the reflection property of integrals and the bound of $0 < x_f < L$ results in the right side of equation (20) becoming

$$(F(t)/\rho A)\left[\int_{-L}^{0} -\delta(-x - x_f) \, e^{-i\lambda_n x} \, dx + \int_{0}^{L} \delta(x - x_f) \, e^{-i\lambda_n x} \, dx\right]$$

$$= -F(t)\varphi_n(x_f)/(\rho A). \tag{22}$$

Equations (21) and (22) can be equated (for $n = m$) to form ordinary differential equations for the generalized co-ordinates b_n as

$$\dot{b}_n(t) - \Lambda_n b_n(t) = -F(t)\varphi_n(x_f)/(4L\Lambda_n \rho A). \tag{23}$$

An explicit solution to equation (23) cannot be found until a time-dependent forcing function has been specified.

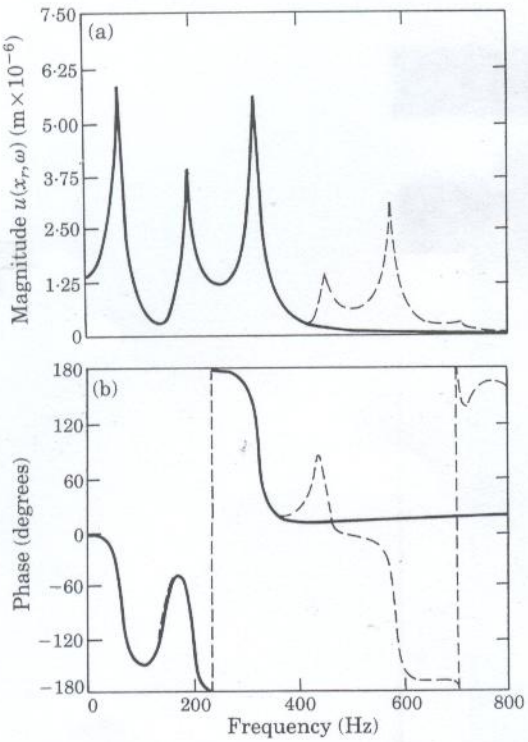

Figure 4. The frequency response of an axially forced beam: (a) magnitude; (b) phase. ——, six-term model, ····, 50-term model.

The initial conditions of the generalized co-ordinates can be determined from the initial conditions of the bar. This equation is

$$b_n(0) = \frac{1}{4\lambda_n^2 L}\int_0^L \frac{\partial u}{\partial x}(x,0)\frac{\mathrm{d}\varphi_n(x)}{\mathrm{d}x}\,\mathrm{d}x - \frac{1}{4\Lambda_n L}\int_0^L \frac{\partial u}{\partial t}(x,0)\varphi_n(x)\,\mathrm{d}x, \tag{24}$$

where $(\partial u/\partial x)(x, 0)$ is the initial strain energy in the bar (dimensionless) and $(\partial u/\partial t)(x, 0)$ is the initial velocity of the bar (m/s). The formulation of equation (24) is presented in the Appendix.

5. FREQUENCY RESPONSE

A frequency domain solution to equation (23) can be found by specifying that the forcing function $F(t)$ be equal to a harmonic function $F_0 e^{i\omega t}$, where F_0 has units of Newtons. Solving the differential equation (23) results in the following solution to the generalized co-ordinates:

$$b_n(t) = \frac{-F_0\varphi_n(x_f)}{(i\omega - \Lambda_n)4L\Lambda_n\rho A}\,e^{i\omega t}. \tag{25}$$

When equation (25) is inserted into equation (12), the displacement of the bar becomes

$$u(x,t) = \sum_{n=-\infty}^{\infty} \frac{-F_0\varphi_n(x_f)\varphi_n(x)}{(i\omega - \Lambda_n)4L\Lambda_n\rho A}\,e^{i\omega t}. \tag{26}$$

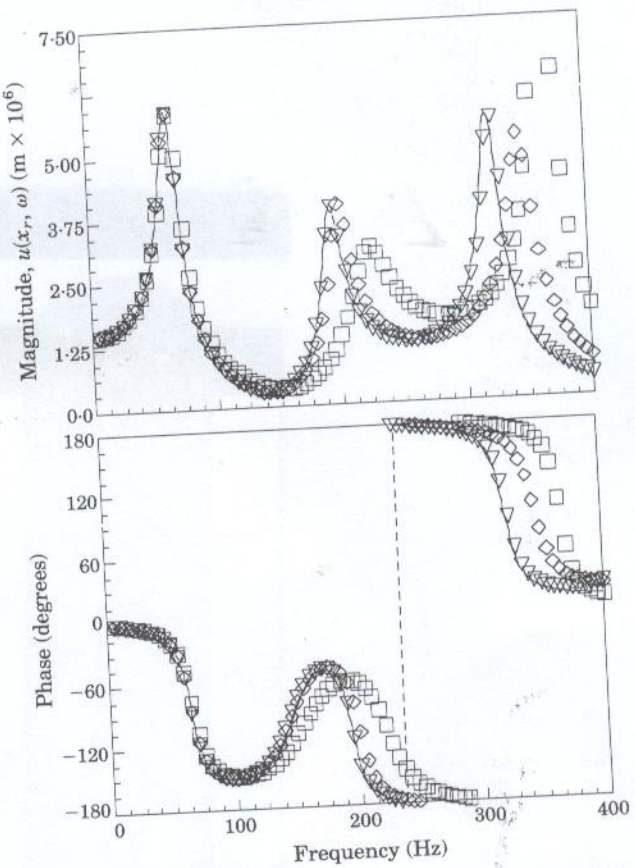

Figure 5. The frequency response of an axially forced beam: (a) magnitude, (b) phase. ——, Six-term continuous model; □, five-node finite element model; ◇, eight-node finite element model; ▽, 21-node finite element model.

Equation (26) can truncated using $2N$ symmetric terms to yield an engineering solution to the problem.

6. A NUMERICAL EXAMPLE

The accuracy of the model and the effects of truncation error were investigated with a numerical example. The following constants were used: $L = 20$ m, $E = 207 \times 10^9$ N/m^2, $\rho = 7{\cdot}8 \times 10^3$ kg/m^3, $F_0 = 1000$ N, $A = 0{\cdot}01$ m^2, $x_f = 3$ m and $c = 75\,000$ Ns/m. The frequency domain response of the structure $u(x_r, \omega)$, viewed at $x_r = 11$ m for a six-term ($-3 \leqslant n \leqslant 2$) and a 50-term ($-25 \leqslant n \leqslant 24$) model, is shown in Figure 4. Numerical simulations suggest that two first order terms are needed to model each bar resonance. There is only a 0·45 percent ($-46{\cdot}9$ dB) difference between the two truncated models up to the third resonance of the bar. The addition of terms to the model does not change its value at the lower frequencies. This is due to the frequency content of each generalized co-ordinate: the lower indexed co-ordinates contain only the lower frequency response and the higher indexed co-ordinates contain only the higher frequency response.

In Figure 5 is shown the six-term frequency response of the structure compared with finite element analysis results, using five-node (squares), eight-node (diamonds) and 21-node (triangles) finite element models. The addition of terms to the finite element model

produces more accurate results at lower frequencies due to the coupling between the nodes in a finite element formulation. Because the bandwidths of the system matrices are greater than one, the mode shapes are not explicit to the analysis, and the addition of terms (nodes) to the analysis can affect the accuracy of many bar resonance modes. The continuous formulation presented above eleminates the problem of banded system matrices by use of an orthogonal solution to decouple the mode shapes of the bar.

7. CONCLUSIONS

The axial response of a bar with a damper at the end can be determined by using separation of variables and by changing the interval of the problem. A truncated series solution can be implemented to approximate the exact dynamic response. The truncation error at lower frequencies is extremely small. This closed form solution is computationally efficient and the eigenvalues and eigenvectors of the system are explicit.

ACKNOWLEDGMENTS

The author wishes to thank Professor Milan Miklavčič of Michigan State University for his help with this problem. The work described in this paper was performed under the Submarine/Surface Ship ASW Surveillance Program sponsored by the Office of Naval Technology.

REFERENCES

1. W. T. THOMPSON 1981 *Theory of Vibration With Applications*. Englewood Cliffs, New Jersey: Prentice-Hall.
2. P. M. MORSE 1948 *Vibration and Sound*. New York: Macmillan.
3. L. MEIROVITCH 1967 *Analytical Methods in Vibrations*. New York: Macmillan.
4. A. BOKAIAN 1988 *Journal of Sound and Vibration* **126**, 49–65. Natural frequencies of beams under compressive axial loads.
5. N. G. STEPHEN 1989 *Journal of Sound and Vibration* **131**, 345–350. Beam vibration under compressive axial load—upper and lower bound approximation.
6. R. S. ENGEL 1991 *Journal of Sound and Vibration* **146**, 463–477. Dynamic stability of an axially loaded beam on an elastic foundation with damping.
7. A. JOSHI and S. SURYANARAYAN 1989 *Journal of Sound and Vibration* **129**, 313–326. Unified analytical solution for various boundary conditions for the coupled flexural–torsional vibration of beams subjected to axial loads and end moments.
8. R. D. COOK 1974 *Concepts and Applications of Finite Element Analysis*. New York: John Wiley.
9. O. C. ZIENKIEWICZ 1983 *The Finite Element Method*. New York: McGraw-Hill.

APPENDIX: INITIAL CONDITIONS OF GENERALIZED CO-ORDINATES

The initial conditions of the generalized co-ordinates can be determined from the initial conditions of the bar. This begins with equation (12), which is

$$u(x, t) = \sum_{n=-\infty}^{\infty} b_n(t)\varphi_n(x). \tag{A1}$$

Equation (A1) is now differentiated with respect to the spatial variable x and evaluated at $t = 0$ to give

$$(\partial u/\partial x)(x, 0) = \sum_{n=-\infty}^{\infty} b_n(0)\lambda_n(e^{\lambda_n x} + e^{-\lambda_n x}) \tag{A2}$$

and differentiated with respect to the time variable t and evaluated at $t = 0$ to give

$$(\partial u/\partial t)(x, 0) = \sum_{n=-\infty}^{\infty} b_n(0)\Lambda_n(e^{\lambda_n x} - e^{-\lambda_n x}). \tag{A3}$$

Equation (A2) is the initial strain energy in the bar and equation (A3) is the initial velocity of the bar. Equation (A2) is multiplied by the wave speed $\sqrt{E/\rho}$ and is added to equation (A3) to yield

$$\sum_{n=-\infty}^{\infty} 2b_n(0)\Lambda_n e^{\lambda_n x} = \left[\sqrt{\frac{E}{\rho}}\frac{\partial u}{\partial x}(x, 0) + \frac{\partial u}{\partial t}(x, 0)\right] \tag{A4}$$

and is subtracted to yield

$$\sum_{n=-\infty}^{\infty} 2b_n(0)\Lambda_n e^{-\lambda_n x} = \left[\sqrt{\frac{E}{\rho}}\frac{\partial u}{\partial x}(x, 0) - \frac{\partial u}{\partial t}(x, 0)\right]. \tag{A5}$$

The interval of equation (A5) is now changed from $[0, L]$ to $[-L, 0]$ by the substitution of $-x$ for x. This equation is

$$\sum_{n=-\infty}^{\infty} 2b_n(0)\Lambda_n e^{\lambda_n x} = \left[\sqrt{\frac{E}{\rho}}\frac{\partial u}{\partial x}(-x, 0) - \frac{\partial u}{\partial t}(-x, 0)\right], \qquad x \in [-L, 0]. \tag{A6}$$

Equations (A4) and (A6) are now combined and the exponential is broken into two terms: one contains the index n and one does not contain the index n. The resulting equation is

$$\sum_{n=-\infty}^{\infty} 2b_n(0)\Lambda_n e^{(2n+1)\pi x i/(2L)}$$

$$= \begin{cases} \left[\sqrt{\frac{E}{\rho}}\frac{\partial u}{\partial x}(-x, 0) - \frac{\partial u}{\partial t}(-x, 0)\right] \exp\left\{\frac{-1}{2L}\log_e\left[\frac{AE\sqrt{\rho} - c\sqrt{E}}{AE\sqrt{\rho} + c\sqrt{E}}\right]x\right\}, & x \in [-L, 0], \\ \left[\sqrt{E\rho}\frac{\partial u}{\partial x}(x, 0) + \frac{\partial u}{\partial t}(x, 0)\right] \exp\left\{\frac{-1}{2L}\log_e\left[\frac{AE\sqrt{\rho} - c\sqrt{E}}{AE\sqrt{\rho} + c\sqrt{E}}\right]x\right\}, & x \in [L, 0]. \end{cases} \tag{A7}$$

The exponential $e^{-(2m+1)\pi x i/(2L)}$ is now multiplied by both sides and the left half of equation (A7) is integrated from $-L$ to L. This yields

$$b_n(0)4\Lambda_n L = \int_{-L}^{0}\left[\sqrt{\frac{E}{\rho}}\frac{\partial u}{\partial x}(-x, 0) - \frac{\partial u}{\partial t}(-x, 0)\right] e^{-\lambda_n x}\,dx$$

$$+ \int_{0}^{L}\left[\sqrt{\frac{E}{\rho}}\frac{\partial u}{\partial x}(x, 0) + \frac{\partial u}{\partial t}(x, 0)\right] e^{-\lambda_n x}\,dx. \tag{A8}$$

Using the reflection property of integrals and equation (11), equation (A8) can be rewritten to give

$$b_n(0) = \frac{1}{4\lambda_n^2 L}\int_0^L \frac{\partial u}{\partial x}(x, 0)\frac{d\varphi_n(x)}{dx}\,dx - \frac{1}{4\Lambda_n L}\int_0^L \frac{\partial u}{\partial t}(x, 0)\varphi_n(x)\,dx. \tag{A9}$$